INTERNATIONAL ATOMIC ENERGY AGENCY
UNITED NATIONS EDUCATIONAL, SCIENTIFIC AND CULTURAL ORGANIZATION

INTERNATIONAL CENTRE FOR THEORETICAL PHYSICS
34100 TRIESTE (ITALY) - P.O.B. 586 - MIRAMARE - STRADA COSTIERA 11 - TELEPHONES: 224281/2/3/4/5/6
CABLE: CENTRATOM - TELEX 46392 ICTP

SMR-30/ 10

WINTER COLLEGE ON ATOMIC AND MOLECULAR PHYSICS

26 January - 18 March 1977

TECHNIQUES OF SOLID-STATE LASERS

(Taken from "Laser devices and techniques")

O. SVELTO

Istituto di Fisica
del Politecnico
Milano

C2 Techniques of Solid-State Lasers

O. SVELTO

Istituto di Fisica del Politecnico
Milano, Italy

Contents

Abstract

This chapter describes several techniques which are important in work with solid-state lasers. These include *Q*-switching, mode selection, and mode locking. In addition, measurement techniques for the study of picosecond pulses and the current knowledge of the properties of these pulses are discussed. The discussion is generally concerned with the principles of operation of these techniques, although for some topics the present state of the theoretical understanding is reviewed as well.

Laser Handbook, edited by
F. T. Arecchi and E. O. Schulz-DuBois

1 *Q-switched lasers*

The technique of Q-switching, first proposed by Hellwarth (1961), is a method enabling one to obtain a sharp single laser pulse with large peak intensity (giant pulses). The principle of the technique is the following. Suppose that a shutter is introduced into the laser cavity. If the shutter is closed, laser action will not occur, and the population inversion can reach very large values. If now the shutter is suddenly opened, the laser will have a gain much in excess of the losses and the energy stored will be released in the form of a short (a few nanoseconds) and intense light pulse. The system indeed works in this way provided the shutter is opened in a time short compared to the build-up time of the laser pulse (fast switch). In the case of slow switching multiple pulses may occur. In a slow switch, in fact, the energy stored within the medium prior to switching is depleted in a series of steps corresponding to the emission of multiple pulses. Each pulse drives the gain below the instantaneous threshold, thus inhibiting further oscillation until the loss of laser cavity and switch have decreased to the new lower threshold.

The following switching systems are more commonly used.

1.1 Electro-optical shutters

They make use of an electro-optical effect such as the Kerr or (more frequently) the Pockels effect. Fig. 1 shows a shutter consisting of a polarizer and a Kerr cell. The Kerr cell is biased and oriented such that it converts the polarization passed by the polarizer into circularly polarized light. After reflection at the mirror, it is reconverted by the Kerr cell to linearly polarized light oriented 90° from the original direction.

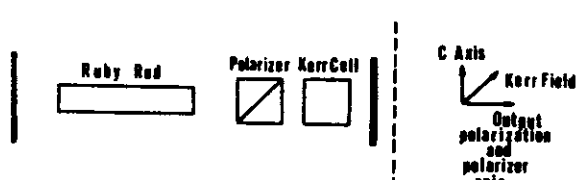

Fig. 1. Polarizer–Kerr-cell combination for Q-switching.

The switch is opened by reducing the bias voltage to zero. The Kerr cell then loses its birefrigence and transmits light without affecting the polarization. A Kerr cell usually requires high bias voltage (10–20 kV). A Pockels cell, which works in the same arrangement, although with linear rather than quadratic electro-optic effect, usually requires a smaller voltage (≈ 5 kV).

1.2 Mechanical shutters

A mechanical means of Q-switching consists in rotating one of the end mirrors (or a 90° roof-top prism) of the laser resonator about an axis perpendicular to the axis of the resonator. If a roof-top prism is used, the rotation axis must be perpendicular to

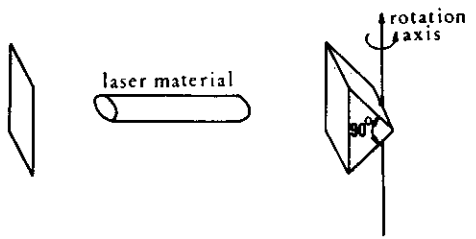

Fig. 2. Rotating roof-top prism system for Q-switching.

the apex line of the prism as shown in fig. 2. To avoid multiple pulses, the rotation speed should be of the order of 30000 rpm (for a resonator length of about 50 cm).

1.3 Shutters using saturable dyes

Suppose one introduces into the laser cavity a saturable absorber whose absorption frequency is coincident with the laser frequency and suppose that the initial (i.e. not bleached) absorption of the absorber is around 50%. Laser action can start only when the gain of the active material compensates for the loss of the saturable absorber plus cavity losses. The population inversion can therefore reach high initial values. When laser action starts, however, the saturable dye is rapidly bleached, while the inversion of the active material is hardly decreased from its initial value. When the saturable dye is bleached the laser will therefore have a gain much larger than the losses and a giant light pulse will develop. The saturable dyes more commonly used are a solution of phthalocyanine in nitrobenzene or cryptocyanine in methanol for ruby lasers, and solutions of polymethine dyes (such as Eastman 9740 or 9860 dyes) for Nd^{3+} lasers. Saturable dyes in the form of a glass filter (e.g. Schott RG10) are also used. The bleaching of these dyes is often interpreted in terms of a two level

system. Their actual behavior is, however, much more complicated, as discussed by several authors, in particular by Giuliano and Hess (1967) for cryptocyanine and by Hercher et al. (1968) for phthalocyanine.

1.4 Q-switching theory

The theory of Q-switching has been treated by several authors, in particular by Vuylsteke (1963) and by Wagner and Lengyel (1963) for the case of a fast switch and by Szabo and Stein (1965) and Erickson and Szabo (1966) for the case in which a saturable dye is used as a Q-switching system. These last authors, however, reach the conclusion that, with the saturable dyes more commonly used, the results are essentially identical to the fast-switch case. Only this last case is therefore discussed here. The following discussion will be based on rate-equations (Statz and De Mars 1960 and Dunsmuir 1961). The theory is similar to that of Wagner and Lengyel (1963) (see also Lengyel 1966 and Hellwarth 1966), except for a somewhat different notation. The following assumption will be made: (i). The relaxation between pump bands and the upper laser level is very fast. (ii). The resonator is made up by two plane parallel mirrors. (iii). The spatial variation of the population inversion due to the standing wave pattern of the mode is neglected. The laser is oscillating in a single mode, whose frequency is coincident with the center of the gain line. Under these assumptions, for the case of a three level system such as ruby, one can write the following rate equations:

$$\dot{n} = \beta(N - n) - 2Bqn - (N + n)/\tau, \quad \dot{q} = (V_a Bn - 1/T)\, q\,. \tag{1a,b}$$

In eq. (1a) n is the population inversion per unit volume, β is a coefficient ($\sec^{-1}$) which is proportional to the pump power (in the following β=const. is assumed), N is the number of active ions per unit volume, B is the coefficient of stimulated emission, q is the total number of photons in the cavity, and τ is the spontaneous decay time of the upper laser level. In eq. (1b) V_a is the volume of the active material and T is the photon decay time due to the losses. The term $V_a Bnq$ in eq. (1b) corresponds to $-2Bqn$ in eq. (1a) since there is a simple balance between the total number of stimulated emission (or absorption) processes and the number of photons produced (or absorbed). An explicit expression for B and T can be obtained in the following way. Consider a wave of intensity I propagating back and forth in the cavity. For small gain and losses the increase in intensity ΔI for a single passage is, in the small signal regime,

$$\Delta I = (\sigma ln - \gamma)\, I\,, \tag{2}$$

where σ is the peak absorption cross section for the laser transition, l is the length of the active material, and γ is the loss per pass.

This increase of intensity will occur in a time $\Delta t = d/c$ where d is the cavity length.

If one divides both sides of eq. (2) by Δt and approximates $\Delta I/\Delta t$ by $\mathrm{d}I/\mathrm{d}t$, one obtains

$$\frac{\mathrm{d}I}{\mathrm{d}t} = \left(\frac{\sigma c l}{d} n - \frac{\gamma c}{d}\right) I . \tag{3}$$

The comparison of eq. (3) with eq. (1b) shows that

$$B = \sigma c l / V_a d = \sigma c / V_c , \quad T = d/c\gamma , \tag{4a,b}$$

where V_c is the cavity volume (usually larger than the volume V_a of the active material). The loss per pass γ may also be written as the sum of a term γ_c due to output coupling and a term γ_i due to internal losses (e.g. due to scattering, diffraction and mirror absorption). Accordingly one may write

$$1/T = 1/T_c + 1/T_i = (c/d)\,(\gamma_c + \gamma_i) . \tag{5}$$

Note that a term to account for spontaneous emission into the laser mode has been omitted from eq. (1b). This term is only necessary to explain the start of the laser oscillation, but it does not appreciably affect the subsequent time evolution of $n(t)$ and $q(t)$.

The inversion n_i reached before switching, can be obtained from eq. (1a) by letting $q=0$. If one assumes that, before switching, the pump is applied for a time long enough to reach steady state, i.e. appreciably longer than τ, one can also set $\dot{n}=0$ in the equation and therefore has

$$n_i = N(\beta\tau - 1)/(\beta\tau + 1) . \tag{6}$$

Eq. (6) can be put in a form more suitable for calculation in the following way. Suppose the laser rod is tested in normal (i.e. not Q-switched) operation between two mirrors of (nominally) perfect reflectivity. If internal losses due to scattering and diffraction are small, the threshold inversion n_c will be much smaller than N. Setting $\dot{n}=0$ and $q=0$ in eq. (1a), one has for the critical pump rate β_c in this case

$$\beta_c = (N + n_c)/(N - n_c)\,\tau \approx 1/\tau . \tag{7}$$

Therefore eq. (6) can be rewritten as

$$n_i = N[(\beta/\beta_c) - 1]/[(\beta/\beta_c) + 1] . \tag{8}$$

In this form the formula allows the evaluation of n_i from the actual pump power (or energy) and the threshold pump power (or energy) of the same rod between two highly reflecting mirrors. Obviously, for $(\beta/\beta_c) \gg 1$ complete inversion can be reached.

Assume now that at time $t=0$ the shutter is suddenly opened. The resulting time evolution of $n(t)$ and $q(t)$ is obtained from eqs. (1) by applying the initial condition $n(0)=n_i$ (it is recalled that an initial small number of photons, e.g. from spontaneous emission, is formally required for the start of the laser oscillation). Neglecting the pump term and the spontaneous decay term in eq. (1a) for $t>0$ one has then to solve

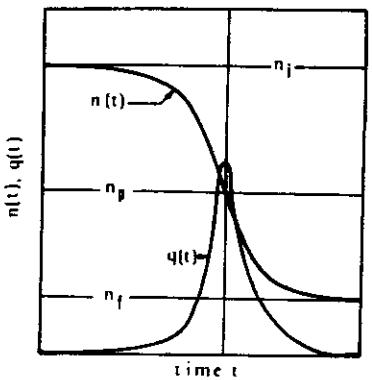

Fig. 3. Typical time evolution of population inversion $n(t)$ and total number of cavity photons $q(t)$ in Q-switching operation (after Lengyel 1966).

the two equations

$$\mathrm{d}n/\mathrm{d}t = -2Bqn, \quad \mathrm{d}q/\mathrm{d}t = (V_a Bn - 1/T)\,q . \tag{9a,b}$$

A typical solution for $n(t)$ and $q(t)$ as obtained by computer is shown in fig. 3. The inversion n_p at the peak of the pulse is obtained from eq. (9b) by letting $\dot{q}=0$. One obtains, with the help of eqs. (4a) and (4b)

$$n_p = 1/V_a BT = \gamma/\sigma l . \tag{10}$$

To solve eqs. (9) it is advantageous to introduce the following dimensionless variables:

$$\eta = n/n_p , \quad \phi = q/n_p V_a , \quad t^* = t/T . \tag{11a,b,c}$$

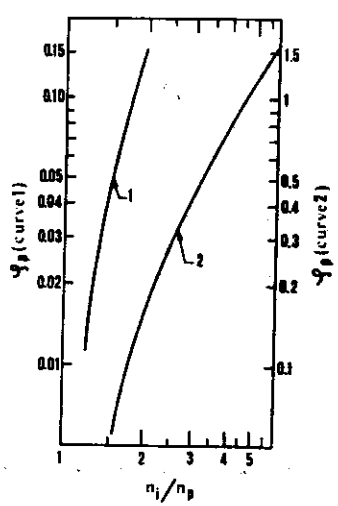

Fig. 4. Plot of normalized peak number of cavity photons ϕ_p vs ratio of initial inversion n_i to the inversion n_p at the peak of the pulse (after Lengyel 1966).

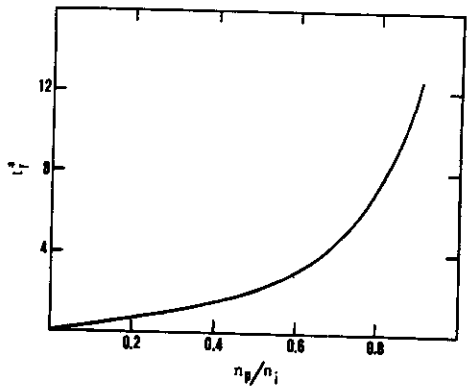

Fig. 5. Plot of pulse risetime t_r^* (normalized to cavity photon decay time) vs n_p/n_i (curve obtained from the numerical data of Wagner and Lengyel 1963, see also Szabo and Stein 1965).

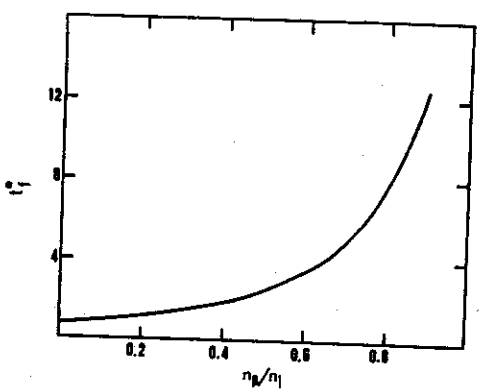

Fig. 6. Plot of pulse fall time t_f^* (normalized to cavity photon decay time) vs n_p/n_i (curve obtained from the numerical data of Wagner and Lengyel 1963, see also Szabo and Stein 1965).

Eqs. (9) then become

$$d\eta/dt^* = -2\phi\eta, \quad d\phi/dt^* = (\eta - 1)\,\phi\,. \tag{12a,b}$$

They should be solved subject to the initial condition $\eta_i = n_i/n_p$ for $t^* = 0$. Eqs. (12) cannot be solved analytically. It is clear, however, that the solution will be of the type $\eta = \eta(n_i/n_p, t^*)$ and $\phi = \phi(n_i/n_p, t^*)$ i.e. it will contain the ratio n_i/n_p as a parameter and will functionally depend on t^* (time in units of the photon decay time). In particular, the peak value ϕ_p and the risetime t_r^* and fall time t_f^* of the pulse will be only functions of n_i/n_p. In figs. 4, 5 and 6 ϕ_p, t_r^*, and t_f^* are respectively plotted vs n_i/n_p. The quantities t_r^* and t_f^* are here defined as the times from the half power point to

the peak or vice versa. It is interesting to note that t_r^* is always smaller than t_f^* i. e. the pulse is asymmetric. The quantity ϕ_p can be obtained analytically by taking the ratio of eqs. (12a) and (12b) and by integrating the resulting equation. One finds

$$\phi - \phi_i = \tfrac{1}{2}[\ln(\eta/\eta_i) - (\eta - \eta_i)], \tag{13}$$

where ϕ_i is the (very small) initial value of ϕ due to spontaneous emission. At the peak of the pulse ($\eta_p = 1$) neglecting ϕ_i one gets from eq. (13)

$$\phi_p = \tfrac{1}{2}[-\ln(\eta_i/\eta_p) + \eta_p(1 - \eta_i/\eta_p)]. \tag{14}$$

The connection between the laser output power P and the photon number q is

$$P = qh\nu/T_c, \tag{15}$$

so that the peak power is

$$P_p = h\nu\phi_p/BT_cT = (h\nu c/d)(V_c/\sigma d)(\gamma\gamma_c\phi_p) \tag{16}$$

The total output energy E is from eqs. (15), (11), and (5)

$$E = (h\nu/T_c)\int_{-\infty}^{+\infty} q\,dt = (\gamma_c/\gamma)h\nu n_p V_a \int_{-\infty}^{+\infty} \phi\,dt^*, \tag{17}$$

where eqs. (11) have been used. The integral of eq. (17) can easily be carried out by integrating both sides of eq. (12b) using the condition $\phi(t^* = \infty) = \phi(t^* = -\infty) = 0$ and eq. (12a). One finds $\int_{-\infty}^{+\infty}\phi dt^* = \frac{1}{2}(\eta_i - \eta_f)$ and, upon substitution of this result in eq. (17)

$$E = \tfrac{1}{2}(\gamma_c/\gamma)h\nu V_a(n_i - n_f) = \tfrac{1}{2}(\gamma_c/\gamma)h\nu V_a n_i(n_i - n_f)/n_i, \tag{18}$$

where n_f is the final inversion left in the active material after termination of the pulse (see fig. 3). Eq. (18) could have been written by inspection from a straightforward energy balance consideration. The quantity $(n_i - n_f)/n_i$ in (18) is in effect an energy utilization factor, since the total available output energy connected with the initial inversion n_i is $\frac{1}{2}h\nu V_a n_i$. The energy utilization factor can be expressed as a function of n_i/n_p by considering eq. (13) for the time $t \to \infty$ [$\phi(\infty) = 0$]. Neglecting ϕ_i one gets

$$(n_i - n_f)/n_i = (n_p/n_i)\ln(n_i/n_f). \tag{19}$$

The energy utilization factor from eq. (19) is plotted vs n_i/n_p in fig. 7.

Finally it is pointed out that, for a given volume V_a of active material, both n_i and n_p do not depend upon the cavity length d. Hence the pulse energy E also is not dependent upon d, as expected. The peak power P_p, however, is inversely proportional to d. This can be seen with the help of eqs. (1) and (4). This result is also expected because the pulse risetime and falltime are proportional to the cavity length.

For lasers using 4-level materials, such as those containing Nd^{3+} ions, a similar theory can be developed. Assuming fast relaxation between pump bands and upper

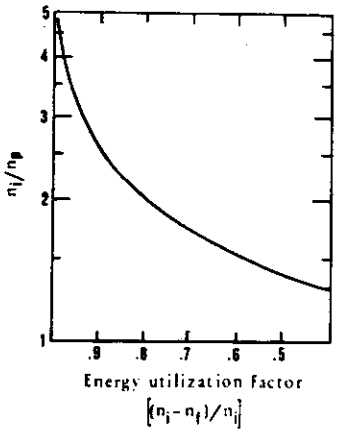

Fig. 7. Plot of the energy utilization factor $(n_i - n_f)/n_i$ vs n_i/n_p (after Lengyel 1966).

laser level, and assuming that the lower laser level is always empty, one can write the following rate equations:

$$\dot{n} = \beta(N - n) - Bqn - n/\tau, \quad \dot{q} = (V_a Bn - 1/T)\, q, \tag{20a, b}$$

where the symbols have the same meaning as before. The inversion before switching is now from eq. (20a) (setting $\dot{n} = q = 0$)

$$n_i = N\beta\tau/(1 + \beta\tau) \tag{21}$$

and the inversion at the pulse peak is from eq. (20b) (setting $\dot{q} = 0$)

$$n_p = 1/V_a BT. \tag{22}$$

If the same laser was operated in normal (i.e. not Q-switched) laser action, the threshold inversion would have been

$$n_c = 1/V_a BT = n_p \tag{23}$$

and the threshold pump rate

$$\beta_c = n_c/(N - n_c)\,\tau. \tag{24}$$

If one assumes that the inversion in normal laser action or in Q-switched operation is always much smaller than N, one may approximate eq. (21) by $n_i = N\beta\tau$ and eq. (24) by $\beta_c = n_c/N\tau$. Using eq. (23) one finds

$$n_i/n_p = \beta/\beta_c \tag{25}$$

which allows a determination of n_i/n_p from the actual pump rate β for Q-switch operation and the pump rate β_c for the normal laser operation.

In the calculation of the evolution of the giant pulse, one would again neglect the pump term and the spontaneous decay term of eq. (20a) and introduce reduced variables:

$$\eta = n/n_p, \quad \phi = q/2n_p V_a, \quad t^* = t/T. \tag{26}$$

It turns out that the resulting two equations are identical to (12). Therefore, all considerations following eqs. (12) and in particular eqs. (14–19) and the results shown in figs. 4–7 are still valid. Notice, however, that the quantity n_i/n_p is now obtainable by eq. (25).

The theory developed so far is open to some critical comments.

1. It applies only to single mode lasers.
2. It does not take into account the spatial variation of the oscillating mode. In particular it does not consider the longitudinal standing wave pattern of the mode. Furthermore, for a gaussian TEM_{00} mode it is difficult to define the transverse dimensions of the cavity volume V to be put into eq. (4a).
3. With high cavity losses the output pulse is released in a few transit times. Strictly speaking, the theory is not valid then and one should treat the problem on a pass by pass basis in the way done, for instance, by Vuylsteke (1963). Nevertheless, an experimental check of the theory by Aswazadurian et al. (1968) for a single TEM_{00} gaussian mode Q-switched ruby laser has shown that one can confidently use the above theory even for high mirror transmissivity (50%).

Before ending this section on Q-switched lasers, it is worthwhile to mention another Q-switching principle first suggested by Vuylsteke (1963), which is called pulse-transmission-mode (PTM) operation. The method involves first Q-switching of the laser with mirrors of 100% reflectivity on both ends of the cavity and then, at the peak of the pulse, a fast switching of the output mirror from 100% to zero reflectivity. In this way the internal energy can be released within a single cavity round-trip time. This type of laser operation was reported by Hook et al. (1966) to give pulse widths of 4 nsec.

2 *Mode selection*

It is relatively easy to get single transverse mode operation of a Q-switched ruby (and also Nd^{3+}) laser with a saturable absorber as Q-switching element. For a laser rod of medium optical quality it is better to choose a resonator with spherical mirrors as shown by Daneu et al. (1966) rather than plane mirrors as used by McClung and Wiener (1965). In fact, spherical mirror cavities are much less sensitive than plane mirror cavities to internal inhomogeneities of the laser material. To improve the transverse mode control, a diaphragm of about 1 mm and a hemispherical configuration may be used as shown by Mikaelian et al. (1967). With high quality rods, even a plane parallel resonator with an additional diaphragm suffices to achieve single

transverse mode operation as shown by Bjorkholm and Stolen (1968). A laser resonator with plane parallel mirrors offers the advantage of an increased mode volume and hence greater available energy from the inverted medium. A configuration which appears to be even less sensitive to imperfections in the laser rod than a spherical mirror configuration is that proposed by Soncini and Svelto (1967) (see also Soncini and Svelto 1968). This special laser cavity consists of two roof-top prisms with roof angle slightly smaller than 90°. It offers interesting advantages:

1. It can withstand high laser intensities without being damaged.
2. The output coupling can be adjusted by means of a frustrated total reflection technique.

The cavity presents the disadvantage, however, that it is more difficult to align than a plane parallel one. As saturable absorbers for ruby, both phtalocyanine in nitrobenzene or cryptocyanine in methanol (or acetone) may be used. Cryptocyanine is less suitable if single longitudinal mode operation is intended.

For single longitudinal mode operation in Q-switching, one may replace one of the cavity mirrors by a suitable resonant reflector such as that of Hercher (1965). However, if the laser is already restricted to oscillation in a single transverse mode, then it usually oscillates in no more than a single longitudinal mode. The restriction to a single longitudinal mode is then caused by a natural mode selection mechanism associated with the dye as pointed out by Sooy (1965). His argument is roughly as follows. Since each mode starts from the same noise level due to spontaneous emission, the ratio P_1/P_2 of the power levels in two modes 1 and 2, after a number of q transits of the light in the cavity, is given by

$$\frac{P_1}{P_2} = \left[\frac{G_1(1-\gamma_1)}{G_2(1-\gamma_2)}\right]^q, \tag{27}$$

where G_1 and G_2 is the gain and γ_1 and γ_2 is the loss per pass of the two modes, respectively. Now, in a Q-switched laser with saturable dye, the total number q of transits for the light to build up from noise level close to the peak value is very high. Clearly, before the dye is bleached, the cavity losses are very high and therefore the light build-up is very slow. Assuming, for simplicity, equal gain for the two modes then according to eq. (27) a very small difference $\gamma_1-\gamma_2$ is sufficient to produce a large power difference between the two modes. A typical value of q, according to the estimates of Sooy (1965) and to the measurements of Daneu et al. (1966), is $q=2000$. From eq. (27) (in the case $G_1=G_2$) a 10 dB mode suppression (i.e. $P_1/P_2=10$) is predicted for $\gamma_1-\gamma_2\approx 10^{-3}$, a very small difference in losses between the two modes indeed. Since such small differences in loss occur naturally, even without any intentional mode selection, it is clear that single mode operation is often obtained with passive Q-switched lasers. As expected for Q-switching by mechanical or electro-optical means, the described mode selection mechanism is not effective. In this case the laser buildup from noise is much faster and q may be of the order of only 10 or 20.

Actually, the discussion of mode selection would call for a more careful analysis. In fact, as will be shown later, saturable dyes are also the standard means to produce

mode-locking which implies a large oscillating bandwidth. This appears to be in contradiction to what has just been said. Although a sufficiently careful analysis has not, to our knowledge, been made, the two different behaviors seem related to the fact that dyes with long relaxation time tend to narrow the spectral width while dyes with fast relaxation times tend to broaden the spectral width of lasers. Therefore, in the case of ruby, phtalocyanine appears to be more suitable than cryptocyanine for Q-switching with a single longitudinal mode output. Other phenomena may, however, also play an important role such as the homogeneous or inhomogeneous character of the dye absorption line. Actually phtalocyanine seems to be homogeneously, and cryptocyanine partially inhomogeneously broadened (see Giuliano and Hess 1967 and Hercher et al. 1968).

The peak output power for a single mode Q-switched ruby laser, according to the references previously cited (McClung and Wiener 1965, Daneu et al. 1966, Mikaelian et al. 1967, Bjorkholm and Stolen 1968) ranges consistently between 1 and 4 MW for rod lengths between 7.5 and 12 cm. The diameter of the spot is usually of the order of 1 mm. For the roof-top prism cavity mentioned above (and probably also for plane or concentric cavities) the spot size is largely determined by the thermal lens effect due to heating of the laser rod by the pump light. For comparison with the above numbers, 100 MW peak power in a 6 mm diameter diffraction limited beam in a single transverse but not single longitudinal mode were obtained by Bortfeld et al. (1964). These authors used a rotating prism Q-switching system and a 3 inch long, $\frac{5}{8}$ inch diameter ruby rod of high optical quality.

The achievement of single longitudinal mode selection in normal, not Q-switched, cw or pulsed laser action for solid state lasers is a much more difficult problem and so far it is not solved in general. A resonant etalon working either in reflection (Kleinman and Kisliuk 1962 and also Roess 1964) or in transmission (Manger and Rothe 1963) was used but with somewhat limited success. Another interesting mode selection system due to Smith (1965) utilizes a Michelson-type interferometer. Two main difficulties must be faced with longitudinal mode selection in solid state lasers:

1. Due to the pump power, the rod expands thermally thus changing the effective cavity length. This phenomenon easily produces mode hopping.
2. The gain linewidth is much larger by at least two orders of magnitude than that of gas lasers.

As a result so far single longitudinal mode operation with solid state lasers was achieved only for pump powers a few percent above threshold.

3 *Mode locking*

In the preceding section it was pointed out that it is difficult to isolate a single longitudinal mode in a solid state laser operation. When many modes are oscillating, the time behavior of the laser output is an irregular, spiking emission since the modes do not usually oscillate with comparable amplitudes and since their phases are more

or less random. Very interesting phenomena occur however, when the modes are forced to oscillate with similar amplitudes and with their phases locked.

As an illustration, let us consider the case of $2N+1$ longitudinal modes which oscillate with the same amplitude E_0. Let us further assume that the phases ϕ_k of the modes are locked according to the relation

$$\phi_k - \phi_{k-1} = \alpha, \tag{28}$$

where α is a constant. The total electric field $E(t)$ of the e.m. wave at any point (inside and outside the resonator) can then be written as

$$E(t) = \sum_{l=-N}^{N} E_0 \exp i[(\omega_0 + l\omega)t + l\alpha] \tag{29}$$

where ω_0 is the center frequency, and ω is the difference frequency between two successive modes. For simplicity, the phase of the center mode is assumed to be zero. For a plane parallel resonator of length d, if cavity dispersion is neglected, ω is a constant and is given by

$$\omega = \pi c/d. \tag{30}$$

The summation of eq. (29) can be carried out with the result

$$E(t) = A(t)\exp(i\omega_0 t), \tag{31}$$

where

$$A(t) = \frac{E_0 \sin[\frac{1}{2}(2N+1)(\omega t + \alpha)]}{\sin[\frac{1}{2}(\omega t + \alpha)]}. \tag{32}$$

$E(t)$ therefore consists of a sinusoidal carrier of the central mode frequency ω_0 whose amplitude $A(t)$ changes with time according to eq. (32). The associated output power is proportional to $A^2(t)$. An example is shown in fig. 8 for $2N+1=7$ oscillating modes.

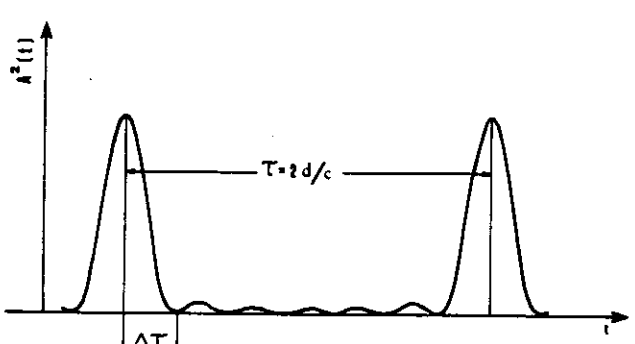

Fig. 8. Time behavior of the squared amplitude of the electric field for the case of 7 oscillating modes with locked phases and equal amplitude.

Due to the phase locking condition (28), the oscillating modes interfere to give short light pulses. The pulse maxima occur at those times when the denominator of eq. (32) vanishes. Two successive pulses are thus separated by a time

$$\tau = 2\pi/\omega = 2d/c. \tag{33}$$

This is the time for a round trip of light in the cavity. The cavity oscillation can therefore also be understood in terms of a pulse which propagates back and forth in the cavity. The time difference $\Delta\tau$ between the peak of the pulse amplitude and its first zero is, from eq. (32)

$$\Delta\tau = 1/\Delta\nu, \tag{34}$$

where $\Delta\nu = (2N+1)\omega/2\pi$ is the total oscillating bandwidth. The full-width between half-power points of $A^2(t)$ is approximately equal to $\Delta\tau$. Therefore, a large oscillating bandwidth is required for obtaining very short pulses. Obviously this bandwidth cannot exceed the gain bandwidth of the laser. Therefore, with typical gas lasers, one cannot get pulses shorter than about 1 nsec. With solid state lasers, however, one may get pulses as short as 1 psec or even less. In addition very large peak powers may be obtained. The peak power is proportional to $(2N+1)^2A_0^2$, whereas for random phases the power is the sum of powers in the modes and hence proportional to $(2N+1)A^2$. The peak power enhancement due to mode locking is therefore equal to the number of oscillating modes, which may typically range between 10^3 and 10^4 for solid state lasers. At the same time, the average power is little or not at all changed by mode locking.

The most commonly used mode-locking systems belong to one of the following two categories:

1. Mode locking by an active modulator which is driven by an external signal.
2. Mode locking by means of a suitable nonlinear optical material (passive mode locking).

To illustrate the first method, suppose there is within the cavity a modulator driven by an external signal, which produces a sinusoidally time varying loss at frequency ω'. If $\omega' \neq \omega$, this loss will simply amplitude modulate every cavity mode. If $\omega' = \omega$, however, every mode will have amplitude modulation side bands which coincide and hence will exchange power with the two neighbouring modes. As a result, the phases of all modes tend to lock. This type of locking, often referred to as AM-type of locking, will not be treated here, since it is more often used for gas lasers. Reference is made to the work by McDuff and Harris (1967) and to more recent ones by Siegman and Kuizenga (1969) and Kuizenga and Siegman (1970a). We only recall that, if dispersion and saturation of the active material may be neglected, mode locking occurs according to eq. (28). In that case the value of α adjusts itself such that the pulse, while travelling in the cavity, traverses the lossy element at the time of minimum loss. There is an alternative way of mode locking by means of an active modulator. It is based on an element within the cavity whose optical path length is

sinusoidally modulated at frequency ω. This type of locking is often referred to as the FM-type of locking. This case is not treated here either and the reader is again referred to the works of Harris and McDuff (1965), Siegman and Kuizenga (1969) and Kuizenga and Siegman (1970a, b). For AM-type of locking both KDP Pockels cells (Deutsch 1965) and ultrasonic standing-wave diffraction cells (Hargrove et al. 1964, De Maria et al. 1966a and DiDomenico et al. 1966) have been utilized. For FM-type of locking, only Pockels cells have been used (Harris and Targ 1964).

To illustrate passive mode locking, let us assume there is a suitable saturable absorber in the laser cavity. It suffices here to idealize the absorber material as a two-level system whose resonant frequency coincides with the laser frequency. To understand how a saturable absorber may produce locking let us consider two adjacent axial laser modes. If two modes oscillate, the interaction of the corresponding fields with the saturable absorber leads to a difference in population between lower and upper level which contains a term oscillating at the difference frequency between the two modes. This term effectively represents a time-varying loss within the cavity and it will therefore couple every mode to its two neighbors. According to this interpretation, one would assume that the position of the saturable absorber cell within the cavity should be of importance. Every mode has a well defined standing-wave pattern. The bleaching of the absorber will be determined by a geometrical superposition of these standing-wave patterns. In addition it is clear that the decay time of the upper state population of the absorber also plays a significant role. Evidently a time varying population difference in the absorber can only be produced if this decay time is faster than the inverse of the mode separation frequency. It should be remembered that a saturable dye also gives Q-switching operation. Consequently the time behavior of the output light will display Q-switching and mode locking together as shown in fig. 9a. This behavior indicates the temporal interference of the oscillating modes. The time behavior of every mode by itself would be as shown in fig. 9b. This passive mode locking is not restricted to the use of saturable dyes. For instance, cells with other non-absorbing liquids such as nitrobenzene have also lead to mode-locking (Comly et al. 1968). In this case locking was interpreted as due to power exchange between modes by Rayleigh-wing scattering. Another example is the mode locking, also referred to as self locking, which is sometimes observed with long laser cavities (>1 m) and which is due to the saturation of the laser material itself (Statz and Tang 1965). A significant advantage of passive mode locking is that with a suitable

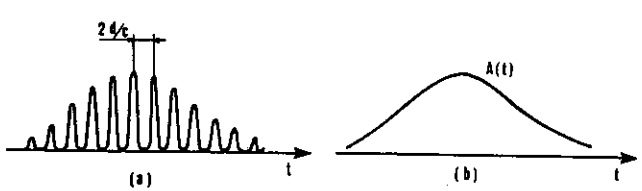

Fig. 9. a) Typical time behavior for the output light of a simultaneously Q-switched and mode-locked laser. b) Corresponding time behavior of each oscillating mode.

nonlinear optical material locking is automatically achieved. On the other hand, mode locking by an active modulator requires the critical adjustment of the modulating frequency to the difference frequency between adjacent modes. Here, however, the laser pulses are synchronous with an external signal, a convenience for certain experimental or practical situations.

As shown before, there is an alternative way of describing mode locking in terms of short light pulses which travel back and forth in the laser cavity. One can therefore follow the propagating pulse through the laser material and the nonlinear element or the active modulator. In the case of cw locking, selfconsistency requires that the pulse remains unchanged after a round trip in the cavity. This point of view was used by Cutler (1955) to analyze an analogous microwave regenerative pulse generator. It turned out to offer a powerful method for analyzing cw locking by means of an active modulator (Siegman and Kuizenga 1969). An analysis based on Cutler's method can also be used to interpret mode locking by a saturable dye, and the analysis is therefore presented below.

The microwave circuit considered by Cutler is schematically shown in fig. 10. It consists of an amplifier, a filter, a delay line and a nonlinear element, called an

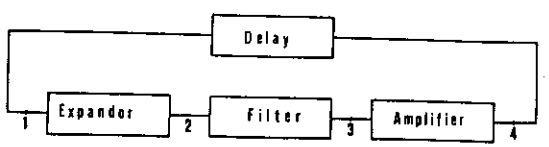

Fig. 10. Schematic diagram of Cutler's pulse regenerative oscillator.

expandor by Cutler, which presents less attenuation for a high-level signal than for a low-level one. When the loop gain exceeds unity, a pulse recirculates indefinitely around the loop and the system behaves as a regenerative pulse generator. The nonlinear element has the effect of shortening the pulse until the pulse width is limited by the filter bandwidth. Let us apply self-consistency to the circuit of fig. 10. If $S_1(t)\exp[i\psi(t)]$ is the signal entering the expandor, the signal leaving the expandor can be written as $S_2(t)=K[S_1(t)]^n\exp[i\psi(t)]$ where K is a constant indicating an amplitude change of the signal, and the superscript n symbolically indicates a general nonlinear operation, not necessarily a power law. Here the nonlinear operation is applied only to the envelope $S_1(t)$, and the effect on the phase function $\psi(t)$ (harmonics of the fundamental frequency) has been neglected. If the filter frequency transmission is called $F(\omega)$, the output $S_3(t)$ from the filter is

$$S_3(t) = (1/2\pi)\int_{-\infty}^{+\infty} F(\omega)\,F_2(\omega)\exp(i\omega t)\,d\omega, \tag{35}$$

where $F_2(\omega)$ is the Fourier transform of $S_2(t)$. The amplifier and circuit losses give a net gain G so that the output of the amplifier is $S_4(t)=GS_3(t)$. The signal $S_5(t)$

from the delay element is delayed by τ. Self-consistency requires that S_5 is equal to S_1 except possibly for an additive phase constant. One thus gets

$$S_1(t)\exp[i\psi(t)] = (1/2\pi)\,GK\exp(-i\theta)\int_{-\infty}^{+\infty} F(\omega)\exp[i\omega(t-\tau)]\,d\omega$$
$$\times\int_{-\infty}^{+\infty}[S_1(t-\tau)]^n\exp[-i\omega(t-\tau)]\exp[i\psi(t-\tau)]\,dt. \tag{36}$$

Given a filter characteristic $F(\omega)$, an expandor nonlinear law n, and a time delay τ, eq. (36) specifies the time function $S_1(t)\exp[i\psi(t)]$. The solution can be given in closed form if the nonlinear operation is actually a power law and if $F(\omega)$ is gaussian. In this case the solution takes the form of a series of gaussian pulses of the type

$$S_1(t)\exp[i\psi(t)] = E\exp[i(\omega_0 t + bt^2)]\exp[-(2t/\Delta\tau)^2], \tag{37}$$

where E is a constant, ω_0 is the center frequency of the filter,

$$b = -\frac{n-1}{n+1}\pi^2\frac{\gamma}{(2/\Delta\omega)^4+\gamma^2} \tag{38}$$

and

$$\Delta\tau = \frac{4}{\pi\Delta\omega(1-1/n)^{\frac{1}{4}}}\left[\frac{2(1+\frac{1}{16}\gamma^2\Delta^4\omega)}{1+\{1+n\gamma^2\Delta^4\omega/4(n+1)^2\}^{\frac{1}{2}}}\right]^{\frac{1}{2}}. \tag{39}$$

In eqs. (38) and (39) $\Delta\omega$ is the bandwidth at the 1 neper points of the filter and γ is the quadratic term of the power series expansion of the loop phase shift

$$\Phi = \alpha + \beta/2\pi(\omega-\omega_0) + [\gamma/(2\pi)^2](\omega-\omega_0)^2 + \cdots. \tag{40}$$

The time separation τ between pulses is

$$\tau = \beta/2\pi, \tag{41}$$

which is identically the group time delay $d\Phi/d\omega$ associated with the phase characteristic at $\omega=\omega_0$. It is interesting to notice that the quadratic term in eq. (40) causes the instantaneous frequency of the pulse to change with time in the form $\nu=\nu_0+bt/\pi$. The popular expression for this is to say that the pulse is chirped.

The preceding analysis may be used to explain mode locking by a saturable absorber. Here the laser medium performs as the amplifier, the linewidth of the laser transition and perhaps of the saturable absorber identify the filter characteristics, the time required for an optical pulse to travel twice the distance between the mirrors defines the loop delay, and the dye serves as the nonlinear element. By comparison with eq. (41) it is readily seen that the pulses are separated by $2d/c$, where d is the cavity length [see eq. (33)]. Note, however, that this result is true only if the

dye cell is placed close to one of the end mirrors, as will be shown later. One also appreciates that the relaxation time of the dye should be shorter than the loop delay of the laser, a condition which was previously introduced in the frequency domain on the basis of cavity modes. To account for dispersion, the refractive index of the media, in particular of the laser material within the feed back loop may be written in the form $n=n_0+(dn/d\omega)(\omega-\omega_0)+\frac{1}{2}(d^2n/d\omega^2)(\omega-\omega_0)^2+\cdots$. The loop phase shift Φ contains a term $2\pi Ln/c$ with L the length of the dispersive medium. Thus the phase shift Φ will in general, similar to eq. (40), contain a term proportional to $(\omega-\omega_0)^2$. Accordingly one should expect a change of the instantaneous frequency within the pulse. This so-called frequency chirp was indeed observed by Treacy (1968) for a mode-locked Nd^{3+} glass laser.

The analogy should not be pushed too far, however. The mode locked laser with a saturable dye cell is a much more complicated system than Cutler's pulse regenerating circuit, for two main reasons:

1. The transmission properties of the active material and of the saturable dye to a short light pulse cannot be described in a simple way (see Arecchi and Bonifacio 1965).
2. The problem is usually a transient one i.e. the laser is simultaneously Q-switched and mode-locked (see fig. 9).

It is difficult to obtain physically meaningful results by analytical techniques in the traveling-wave approach, although interesting results were obtained by computer calculations (Fleck 1968). An alternative approach which can be handled by analytical techniques and, at the same time, gives some physical insight is to describe the laser in terms of coupled modes. This point of view was adopted by several authors (Sacchi et al. 1967, Kuznetsova et al. 1967, Tang and Statz 1967, Statz et al. 1967, Schwarz 1968). Most of these authors, however, use the socalled 'maximum emission principle' which unfortunately is not generally valid (Schwarz and Gordon 1969). We therefore follow the analysis of Sacchi et al. (1967). This work considers the interaction of just three adjacent modes in the rate equation approximation. Otherwise it closely follows the well known laser theory by Lamb (1964). The linearly polarized field $E_l(r,t)$ associated with the cavity mode of the nominal frequency ω_l is written $E_l(r,t)=\frac{1}{2}[A_lU_l(r)\exp(i\omega_l t+\phi_l)+\text{c.c.}]$. Here $A_l(t)$ describes the time evolution of the field amplitude, and $U_l(r)$ is the space dependent part of the mode functions. These are assumed to form a normalized orthogonal set so that $\int U_l(r)\,U_m(r)\,dV=\delta_{l,m}$, where the integral is over the cavity volume. Finally $\phi_l(t)$ describes the time evolution of the phase. Nonlinear polarization terms of the dye are retained only up to third power in E. It is further assumed that the three amplitudes are equal, $A_l(t)=A(t)$. Then one arrives at two equations for the rate of change of amplitude and phase:

$$2\dot{A} = \left(\frac{1}{T_g}-\frac{1}{T_l}-\frac{1}{T_a}\right)A + A^3[C_1+\xi C_2\cos(\phi_{l-1}-2\phi_l+\phi_{l+1})], \tag{42a}$$

$$\dot{\phi}_l = \left(\frac{\mu}{\hbar}\right)^2\frac{T_1}{T_a[1+(\omega T_1)^2]}A^2\xi\sin(\phi_{l-1}-2\phi_l-\phi_{l+1}). \tag{42b}$$

In eq. (42a) T_g is the photon risetime due to the gain of the laser material. According to eq. (4b) it is given by $T_g = d/c\gamma_g$, where γ_g is the gain per pass. T_1 is the photon decay time due to cavity losses γ_1 ($T_1 = d/c\gamma_1$), T_a is the photon decay time due to the unsaturated losses γ_a of the absorber ($T_a = d/c\gamma_a$), and C_1 and C_2 are positive constants whose magnitude is not relevant for the present qualitative consideration. In eq. (42b) μ is the electric dipole moment of the dye, T_1 is the relaxation time of dye population, ω is the frequency difference between adjacent modes, and ξ is a parameter which describes the mode overlap in the dye cell. This parameter is given by

$$\xi = \int_{\text{cell}} U_{l-1} U_l^2 U_{l+1}\, dV \Big/ \int_{\text{cell}} U_l^2\, dV, \tag{43}$$

with integrals taken over the dye cell.

Eq. (42a) permits a simple interpretation. As soon as the gain γ_g of the laser material exceeds the total losses ($\gamma_1 + \gamma_a$) of the cavity, the field amplitude A will increase exponentially from noise level. Once the cubic term is appreciable, it will increase even faster due to the saturation of the dye. Of course, the growth of $A(t)$ will eventually be limited by gain saturation which is not accounted for in the equation. Due to gain saturation $A(t)$ will reach a maximum and then decreases as shown in fig. 9b. Now dye saturation occurs at much lower power level than gain saturation. Therefore eq. (42a) correctly describes the early rise of the pulse of fig. 9b. Eq. (42b) shows that, as soon as the dye starts to saturate, the rate of change of the phase ϕ_l depends upon the phases ϕ_{l-1} and ϕ_{l+1} of the two adjacent modes. The expression is particularly simple because it considers the interaction of just three modes. By the same token it permits some physical insight into the mechanics of mode locking. The equation has two stationary solutions for the phase ϕ_l, namely

$$\phi_{l-1} - 2\phi_l + \phi_{l+1} = 2n\pi \tag{44a}$$

$$\phi_{l-1} - 2\phi_l + \phi_{l+1} = (2n+1)\,\pi \tag{44b}$$

where n is an integer. It can be shown that the stable solution is (44a) if $\xi > 0$ whereas it is (44b) if $\xi < 0$. To prove that, assume the phase ϕ_l differs by a small amount $\delta\phi_l$ from its stationary value. From eq. (42b) one then obtains

$$\delta\dot{\phi}_l = \mp\, \xi\, \frac{2\mu^2 T_1 A^2}{T_a \hbar^2 [1 + (\omega T_1)^2]}\, \delta\phi_l. \tag{45}$$

Here the $-$ or $+$ sign applies if the presumed stationary solution is (44a) or (44b), respectively. Therefore for $\xi > 0$, $\delta\phi_l$ decreases toward zero if eq. (44a) holds for the stationary phases. Conversely if $\xi < 0$, $\delta\phi_l$ decreases toward zero if eq. (44b) holds. From eq. (45) one sees that, after a momentary deviation from perfect locking, the phases will approach locking in a time t_0 of the order of

$$t_0 = \frac{T_a \hbar^2 [1 + (\omega T_1)^2]}{2\xi \mu^2 T_1 A^2}. \tag{46}$$

For mode locking to occur this time must be much shorter than the risetime of the pulse $A(t)$. Note that t_0 is not a constant since eq. (46) contains A^2 which by itself is time dependent. The formula is nevertheless useful to indicate the effect of a long dye recovery time T_1. Assuming $\omega T_1 \gg 1$, t_0 becomes very long and mode locking does not occur.

Next it is interesting to consider the sign of ξ. For this purpose the mode functions U_l are approximated by standing plane waves, a reasonable simplification for a plane-parallel resonator. Let z be the coordinate along the resonator axis with the origin at one of the mirrors. Then

$$U_l = (2/V)^{\frac{1}{2}} \sin(l\pi z/d), \tag{47}$$

where V is the cavity volume and $(2/V)^{\frac{1}{2}}$ is the normalization constant which insures that $\int U_l^2\, dV = 1$. Assuming a dye cell which is much longer than the optical wavelength, but much shorter than the cavity length, one obtains from eqs. (43) and (47)

$$\xi = (1/2V)\,[2\cos(2\pi z_0/d) + 1], \tag{48}$$

where z_0 is the coordinate position of the dye cell. The equation shows that for a location of the dye cell near either of the cavity mirrors, $z_0 = 0$ or $z_0 = d$, ξ reaches a maximum positive value. Consequently the stable solution for the phases is (44a). Apart from an unessential integral number of 2π the latter equation is equivalent to eq. (28). Both equations indicate mode locking such that two successive pulses of the output train are separated in time by $2d/c$ and only one pulse propagates back and forth in the cavity as shown in fig. 11a. When the dye cell is placed at the cavity center ξ reaches the largest negative value. The stable solution for the phases then becomes (44b). In this case (Sacchi et al. 1967) two successive pulses of the mode-locked output train are separated in time by d/c and two identical pulses propagate in the cavity so that they meet at the center in the dye (fig. 11b). This result can also be understood on the basis of the so-called 'maximum emission principle' (Garmire and Yariv 1967). If the

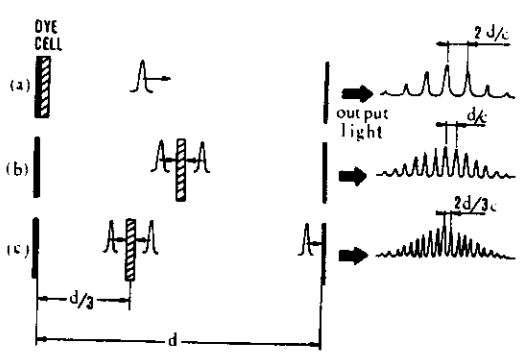

Fig. 11. Pictorial view of pulses propagation inside and outside the laser cavity for three different positions of the dye cell.

dye cell is placed at $\frac{1}{3}$ of the cavity length, $z_0 = \frac{1}{3}d$ or $z_0 = \frac{2}{3}d$, eq. (48) would give $\xi = 0$ and one would not expect any phase locking at all. This is true, however, only for the interaction of three modes. On the other hand, if many modes interact (Kuznetsova et al. 1967), pulses tend to occur which are separated in time by $\frac{2}{3}d/c$. This means that three pulses propagate in the cavity and two of them always meet at the dye (fig. 11c). These results are in agreement with experimental observations (Harrach and Kachen 1968). It should be mentioned, however, that mode-locking is most easily achieved in practice when the dye cell is at one cavity end. This is in fact predicted by the present theory, since ξ reaches its greatest possible absolute magnitude (and therefore t_0 its minimum one) for the dye cell at this position.

This section is concluded by mentioning a few experimental results on mode-locking of solid state lasers. For more detailed information the reader is referred to a very good review paper of DeMaria et al. (1969). Mode locking has been achieved in Nd^{3+}:glass (DeMaria et al. 1966a, b) ruby (Deutsch 1966, Mocker and Collins 1965, Mack 1968, Cubeddu et al. 1969), and Nd^{3+}:YAG (DiDomenico et al. 1966, Clobes and Brienza 1969) lasers either by active modulators or by saturable dyes. The length of the active material usually ranges between 5 and 10 cm, although rods as long as 1 m have been also used. To obtain reliable mode locking, it is recommended to have all interfaces within the laser cavity, such as rod and dye cell end faces, oriented at the Brewster angle. To avoid multiple pulsing, the dye cell should be placed as close as possible to one of the cavity mirrors (Weber 1968a). An alternative approach for the suppression of multiple pulsing is to use a circulating three mirror cavity (Krasyuk et al. 1968) or a special roof top prism cavity (Cubeddu et al. 1969). Both Kodak 9860 in dichloroethane and Kodak 9740 in chlorobenzene have been used as saturable dyes for Nd^{3+}:glass and Nd^{3+}:YAG. Kodak 9860 has an upper limit of the relaxation time T_1 of 6 to 9 psec (Scarlet et al. 1968) and Kodak 9740 an upper limit of 25 to 35 psec (Shelton and Armstrong 1967). For ruby, cryptocyanine in acetone or dicarbocyanine iodide (DDI) in methanol appear to be the best dyes (Mack 1968). Acetone is a more suitable solvent than methanol for cryptocyanine since the peak absorption line of this dye-solvent combination coincides with the ruby line. Recent measurements (Duguay and Hansen 1969a) give a value of $T_1 = 22$ psec for cryptocyanine and $T_1 = 14$ psec for DDI when dissolved in either acetone or methanol. It is not known at present whether the absorption line of the dyes mentioned is homogeneously or inhomogeneously broadened, although the measurements of Hercher et al. (1968) seem to indicate an at least partially inhomogeneous broadening. The position of the active material within the cavity was found to be not critical.

For some applications a single ultrashort light pulse only is required rather than a train. This can be obtained by combining mode locking with the previously described PTM technique (Penney and Heynau 1966, Michon et al. 1966, DeMaria et al. 1967, Basov et al. 1968). A schematic diagram of such a system is shown in fig. 12. The reflectivity of both mirrors M_1 and M_2 is high, and a dye cell is used for mode locking. The Kerr cell polarizer combination is used to achieve the PTM operation. The Kerr cell is initially unenergized, and the polarizing Glan prism is adjusted for maximum

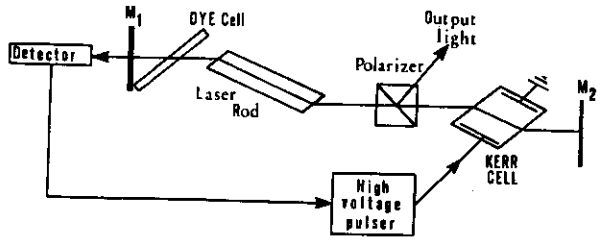

Fig. 12. Schematic diagram of a system which is used to obtain a single output pulse from a mode-locked laser.

transmission. When mode locking occurs, the leakage radiation from one of the mirrors triggers a high-voltage pulser as soon as the optical pulse amplitude reaches a predetermined value. The Kerr cell is then biased by a pulse of its $\frac{1}{4}\lambda$ voltage. Hence the linearly polarized light from the polarizer is converted by the Kerr cell into circularly polarized light. After reflection from the mirror M_2, the Kerr cell reconverts it to linearly polarized light, however, with an orientation of 90° from the original direction. Consequently it is completely coupled out by the polarizer. Instead of a Kerr cell, a Pockels' cell may also be used. For the generation of a single picosecond pulse, the polarization switch and Glan polarizer can also be placed outside the cavity. This latter configuration requires a $\frac{1}{2}\lambda$ voltage across the polarizing switch. It is preferred when the minimum possible pulse width is desired (Basov et al. 1968, Kachen et al. 1968, Von der Linde et al. 1970).

4 *Measurement of picosecond pulses*

Picosecond light pulses cannot, at present, be measured by direct electronic methods, although there is some hope that this will be possible in the not too distant future. The fastest system known today uses a high-speed electron-optical streak camera (Korobkin and Schelev 1968, Bradley et al. 1971) whose present time resolution is about 5 psec. Therefore, picosecond pulses are at present usually measured by less direct optical methods based on a suitable nonlinear optical effect. The methods originally proposed and employed (Weber 1967, Armstrong 1967, Maier et al. 1966) used second harmonic generation in suitable crystals. For instance, the method proposed by Weber (1967) is as follows. The pulse to be measured is first divided into two pulses of orthogonal polarizations (x and y). One of the pulses is delayed by a variable time τ relative to the other. The two pulses are made collinear and then sent to a nonlinear optical crystal, for example ADP. The orientation of the crystal is chosen so that the second harmonic polarization of the crystal is proportional to $E_x E_y$. The output signal $S(\tau)$ at the second harmonic frequency is measured by a detector having a slow response time compared to the duration of the pulse. The resulting signal

$$S(\tau) \propto \int_{-\infty}^{+\infty} E_x^2(t)\, E_y^2(t-\tau)\, \mathrm{d}t \tag{49}$$

is a measure of the overlap of the two pulses. Roughly speaking, if the two pulses are delayed by a time τ larger than their pulse widths, $S(\tau)$ will drop to zero. The measurement of the function $S(\tau)$ therefore allows some conclusions concerning the pulsewidth. For example, for gaussian pulses $E^2 \propto \exp(-2t/\Delta\tau)^2$ where $\Delta\tau$ is the pulse duration of E^2 between 1-neper points, one gets from eq. (49) $S(\tau) \propto \exp -(2\tau^2/\Delta\tau^2)$, so that the width between 1-neper points of $S(\tau)$ is $2^{\frac{1}{2}}\Delta\tau$. Since a separate laser shot is required for every data point and since most lasers are not completely reproducible from shot to shot, some normalization is required. A convenient way of normalization is to take a part of the same pulse by a beam splitter and let it alone produce second harmonics in a second crystal. The signal output of this second crystal S' will be proportional to $\int_{-\infty}^{+\infty} E^4(t)\, \mathrm{d}t$, so that the ratio of S to S' gives a normalized function $G^{(2)}(\tau)$

$$G^{(2)}(\tau) = \int_{-\infty}^{+\infty} E^2(t)\, E^2(t-\tau)\, \mathrm{d}t \Big/ \int_{-\infty}^{+\infty} E^4(t)\, \mathrm{d}t, \tag{50}$$

which in principle is independent of amplitude fluctuations of the pulse from shot to shot. Since $E^2(t)$ is proportional to the field intensity $I(t)$, the function $G^{(2)}(\tau)$ can also be written

$$G^{(2)}(\tau) = \langle I(t)\, I(t+\tau)\rangle / \langle I^2(t)\rangle, \tag{50a}$$

where $\langle\ \rangle$ denotes time averaging. $G^{(2)}(\tau)$ is known as the normalized second order correlation function of $I(t)$. This scheme requires a considerable number of laser shots for one measurement. Unfortunately this enhances the uncertainty of the measured result, since with most lasers the pulse duration appears to vary somewhat from shot to shot.

A measuring method which requires only one shot (Giordmaine et al. 1967, Rentzepis and Duguay 1967) uses a two-photon absorption-fluorescence technique. A schematic diagram of the experimental arrangement is shown in fig. 13. The incoming pulse $E_0(t)$ is split by the beam splitter 1 into two pulses E_1 and E_2 which then meet in a cell containing a suitable two-photon absorption dye. Since two photon

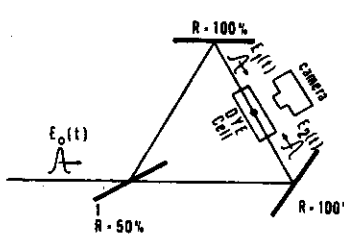

Fig. 13. Measurement of the width of short light pulses by the two-photon absorption-fluorescence technique.

absorption is a nonlinear process, the fluorescent emission of the dye will be strongest in the spatial region where the two pulses overlap. A measurement of this spatial region will give a measure of the width of the incoming pulse. Roughly speaking the extension Δz of this spatial region will be of the order of $c\Delta\tau$, where $\Delta\tau$ is the pulse duration and c the velocity of light. If $\Delta\tau = 1$ psec, one gets $\Delta z = 0.3$ mm, a quantity which can be easily measured. For a better calculation one expresses the total electric field $E(z, t)$ in the dye

$$E = E_1(t - z/c)\sin(kz - \omega t) + E_2(t + z/c)\sin(kz + \omega t) \tag{51}$$

as the sum of the two incoming pulse fields. The origin of z-axis is chosen as the point where the maxima of the two pulses meet. For present purposes c is the group velocity of the two pulses in the dye. The total fluorescent energy at a point z of the dye serves as the measurable spatial signal $S(z)$. This signal is proportional to

$$S(z) \propto \langle E^4\rangle. \tag{52}$$

Averaging in time over a few optical cycles or more and in space over a few optical wavelengths are indicated since the signal is usually recorded on photographic film. From eq. (51) the signal is proportional to

$$S(z) \propto \int_{-\infty}^{+\infty} E_1^4(t - z/c)\, \mathrm{d}t + \int_{-\infty}^{+\infty} E_2^4(t + z/c)\, \mathrm{d}t + 4\int_{-\infty}^{+\infty} E_1^2(t - z/c)\, E_2^2(t + z/c)\, \mathrm{d}t. \tag{53}$$

For the most important case $E_1(t) = E_2(t) = E(t)$, $S(z)$ can be normalized with respect to $S' \propto 2\int_{-\infty}^{+\infty} E^4(t - z/c)\, \mathrm{d}t$ with the result

$$S(\tau)/S' = 1 + 2G^{(2)}(\tau). \tag{54}$$

Here $\tau = 2z/c$ and $G^{(2)}$ is given by eq. (50a). Obviously for $\tau = 0$ $G^{(2)}(0) = 1$ so that $S(0)/S' = 3$. Outside the overlap region of the two pulses, $G^{(2)} = 0$ so that $S/S' = 1$.

For a perfectly mode-locked laser, the photograph of a two-photon absorption and fluorescence experiment shows a trace corresponding to the propagation of both laser pulses without overlap. On a relative scale, the contrast there may be defined as 1. In addition, a brighter spot is recorded at the location where both pulses collide. At its brightest point, the contrast should be 3 on the same scale. The extension of the bright spot in propagation direction is a measure for the pulse duration. For example, for a gaussian pulse $I(t) \propto \exp(-4t^2/\Delta\tau^2)$, after subtraction of the background contrast of 1, the spot will have a width between 1 neper points of $\Delta z = c_0\Delta\tau/n\sqrt{2}$ where c_0 is the vacuum velocity of light and n is the refractive index of the dye liquid (group velocity is here approximated with phase velocity).

Actually, as pointed out by Weber (1968b) and Klauder et al. (1968), the two-photon fluorescence technique requires some caution. In fact if a noise signal of spectral bandwidth $\Delta\omega$ is sent to the measuring apparatus of fig. 13, a brighter spot of a width corresponding to the coherence time $\tau_c = 2\pi/\Delta\omega$ will also appear at $z = 0$.

Therefore the proper interpretation of the bright line strongly depends on the contrast ratio. For an ideally mode-locked laser the ratio should be 3:1 as shown. For a noise signal, such as the light emitted by a free running laser, the contrast ratio is 3:2. To prove this, it is noted that just as for the mode-locked laser, here too one finds $S(0)/S'=3$. At variance with the mode-locking case, however, here one does not have $G(\tau)\neq 0$ for large delay. In the present case, when $\tau>\tau_c$, $I(t)$ and $I(t+\tau)$ are statistically independent so that

$$G^{(2)}(\tau)=\langle I(t)\rangle\langle I(t+\tau)\rangle/\langle I^2(t)\rangle=\langle I\rangle^2/\langle I^2\rangle \quad \text{for} \quad \tau>\tau_c. \tag{54a}$$

It is known that a random or gaussian signal is described by the probability distribution $p(I)=\exp(-I/I_0)$ where $p(I)\,\mathrm{d}I$ is the probability of observing the intensity I in the interval $\mathrm{d}I$, and I_0 is the average intensity. One then has $\langle I\rangle^2=I_0^2$ and $\langle I^2\rangle=2I_0^2$ so that $G^{(2)}=\frac{1}{2}$ for $\tau>\tau_c$. Then from eq. (54) we have $S(\tau)/S'=2$ for $\tau>\tau_c$, hence the contrast ratio is 3:2 as stated above. For an ideal single mode FM laser no bright spot should appear at all, since the technique is not phase sensitive. Experimentally, with long dye cells of about 5 cm a contrast ratio near 2:1 was measured with mode-locked Nd:glass lasers in most of the early work (Klauder et al. 1968). More recently, a sharp spike reaching a contrast ratio 2.5:1 has been observed (Bradley et al. 1969). With very short dye cells of about 50 μm, however, the expected 3:1 contrast ratio was recently obtained (Shapiro and Duguay 1969, Clobes and Brienza 1969). The reason for this disagreement is not completely known. It is possible that long cells affect the incoming pulses*. It is also clear that the theoretical 3:1 contrast ratio is expected only for very accurate alignment of the optical path. The two-photon absorption fluorescence technique also presents other disadvantages:

1. For a train of pulses the bright spot gives information about the average pulsewidth only. By contrast a variation of pulse duration with time within the mode-locked pulse train was observed, at least in some cases (Glenn and Brienza 1967).
2. The technique is able to measure the second order correlation function $G^{(2)}(\tau)$ only which is necessarily symmetrical in the sense $G(\tau)=G(-\tau)$, see eq. (50). As a result the technique is not able to identify pulse asymmetries. This limitation, however, is common to all methods relying on second harmonic generation. On the other hand, the simplicity of the two-photon absorption-fluorescence technique is one of its major advantages provided a measurement of the contrast ratio is not required. Rhodamine 6G in dichloroethane or in ethanol is now commonly used for Nd^{3+} or ruby lasers, respectively (DeMaria et al. 1969). This dye has a strong two-photon fluorescence, and it has the additional advantage that it can be used for both Nd^{3+} and ruby lasers. This is due to the fact that Rhodamine 6G happens to have two absorption bands which are approximately centered at the second harmonic frequencies of Nd^{3+} and ruby, respectively.

* Note added in proof. A more likely explanation is that the very short dye cell system is a more sensitive one since a phototube rather than a photographic film is used to record the fluorescent light. Accordingly, one can use a much lower intensity of the beam, thus avoiding saturation of the dye fluorescence, which, at least for ruby light, has been shown to occur (Bradley et al. 1970c).

Second harmonic generation (SHG) and two-photon fluorescence (TPF) are presently the most popular methods for pulse duration measurements in the picosecond range. Other methods were also developed, however. For example, one may split the beam into two beams which cross at a slight angle. The two beams are then incident on a suitable nonlinear surface such as a photographic film with sensitivity at the two-photon frequency (Burnham and Billman 1968) or a nonlinear photoelectric surface (Burnham 1970). This method, too, gives the second order correlation function $G^{(2)}(\tau)$. Methods which give the third order correlation function $G^{(3)}(\tau_1,\tau_2)=\int I(t)\,I(t+\tau_1)\,I(t+\tau_2)\,\mathrm{d}t$ were also suggested (Weber and Dändliker 1968). The measurement of $G^{(3)}$ was also achieved by three-photon fluorescence (Rentzepis et al. 1970). A method using third harmonic generation in a phase-matchable dye solution was proposed (Bey et al. 1968) and demonstrated (Eckardt and Lee 1969). This method measures the symmetrized function $G^{(3)}(0,\tau)+G^{(3)}(0,-\tau)$. The importance of the measurement of $G^{(3)}(\tau_1,\tau_2)$ stems from the fact that from a knowledge of $G^{(2)}$ and $G^{(3)}$ the time behavior of the intensity $I(t)$ can be deduced (Blount and Klauder 1969).

Even if this information were available, one often would like to obtain additional data, however. Assume $E(t)=A(t)\exp\mathrm{i}[\omega t+\psi(t)]$ is the electric field of an incident laser pulse. The methods based on intensity correlation functions give information only on the amplitude $A(t)$ and no information on $\psi(t)$, the phase modulation of the pulse. A system which at present gives the most complete information about the incoming laser pulse is the so-called dynamic spectrogram introduced by Treacy (1970a, b). The idea is as follows. Suppose one lets the pulse pass through a narrow band filter of bandwidth $\Delta\omega$ centered at ω. If

$$E(t)=\int_{-\infty}^{+\infty} g(\omega)\exp\{-\mathrm{i}[\omega t-\phi(\omega)]\}\,\mathrm{d}\omega, \tag{55}$$

is the electric field of the incident pulse, the pulse after the filter will be given by

$$E'(t)=\int_{\omega-\frac{1}{2}\Delta\omega}^{\omega+\frac{1}{2}\Delta\omega} g(\omega)\exp\{-\mathrm{i}[\omega t-\phi(\omega)]\}\,\mathrm{d}\omega. \tag{56}$$

If $\Delta\omega$ is sufficiently small, $g(\omega)$ will essentially be a constant over the integration range. Then the maximum of the amplitude of $E'(t)$ occurs when the phase $\omega t-\phi(\omega)$ is stationary, i.e. when $\partial[\omega t-\phi(\omega)]/\partial\omega=0$. The time t_M of the pulse maximum is therefore given by

$$t_M=\partial\phi(\omega)/\partial\omega, \tag{57}$$

where the derivative clearly should be taken at the center frequency of the filter. The width Δt of the output pulse $E'(t)$ will be approximately given by $\Delta t=2\pi/\Delta\omega$. Let now the input pulse be simultaneously sent to a series (1, 2, 3...) of narrow band filters with linearly increasing central frequency as shown in fig. 14a. After the filters, one will have a series of pulses with different delays according to eq. 57. As an

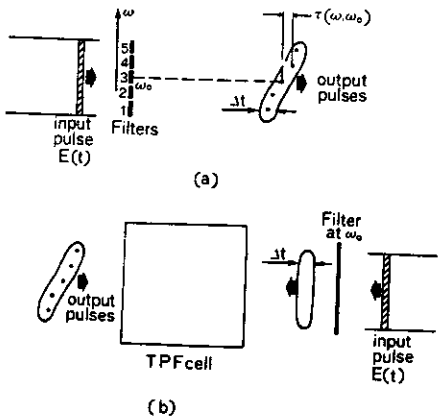

Fig. 14. Working principle of the dynamic spectrogram.

example, in fig. 14a the maxima of the pulses are indicated by dots. The time delay $\tau(\omega, \omega_0)$ between the maximum of the pulse with frequency ω and the maximum at another frequency ω_0 will be

$$\tau(\omega, \omega_0) = [\partial\phi(\omega)/\partial\omega]_\omega - [\partial\phi(\omega)/\partial\omega]_{\omega_0}. \tag{58}$$

Assuming $\tau(\omega, \omega_0)$ is known, integration of eq. (58) yields $\phi(\omega)$ except for a constant and linear term in ω which are not relevant. For a measurement of $\tau(\omega, \omega_0)$ the different output pulses of fig. 14a are made to meet the pulse from the filter at ω_0 in a two-photon-fluorescence (TPF) cell (fig. 14b). One thus obtains a fluorescent track in the cell whose shape is equal to that of the output pulses of fig. 14, and from which $\tau(\omega, \omega_0)$ can be measured. Since the amplitude $g(\omega)$ in eq. (55), or rather its absolute square, can be measured by an ordinary spectrograph, the simultaneous measurement of a static and dynamic spectrogram gives both $g(\omega)$ and $\phi(\omega)$. In this way the electric field amplitude of the incident pulse may be completely measured.

5 *Properties of picosecond pulses*

By using the methods just described, pulse-widths ranging between 2.5 and 15 psec were measured for Nd^{3+}:glass mode-locked lasers. The shortest pulses were obtained with very thin dye cells of about 30 μm (Bradley et al. 1970a). Pulse-widths of about 20 psec were also measured for Nd^{3+}:YAG mode-locked lasers (Clobes and Brienza 1969). In the case of Nd^{3+}:glass, the oscillating bandwidth is quite large (100–200 Å) so that, if the whole bandwidth were locked, the pulse width should be as small as 4.10^{-13} sec from eq. (34). This is an order of magnitude shorter than the experimental observations. This discrepancy was at least partially resolved by recent observations of a subpicosecond structure (Shapiro and Duguay 1969, Bradley et al. 1969, Eckardt

and Lee 1969) and of a linear component of the frequency sweep (Treacy 1968, Treacy 1969) in the output of mode-locked Nd:glass lasers. In the case of ruby, pulses as short as 4 psec were obtained (Mack 1968, Cubeddu et al. 1969). Since in this case the time-bandwidth product $\tau\Delta\nu$ is about unity, no appreciable subpicosecond structure and frequency chirp are expected. The linear component of the frequency sweep can be compensated by a dispersive optical delay line such as the two-grating system suggested by Treacy (1968, 1969). In this way, pulse structures as short as the theoretical limit of 4.10^{-13} sec have been obtained for a Nd:glass laser. To our knowledge, these are the shortest pulses obtained anywhere. To realize even shorter pulses, frequency modulation and subsequent compression of laser pulses was proposed (Giordmaine et al. 1968, Gires and Tournois 1964, Fisher et al. 1969). Although the validity of this technique was demonstrated experimentally in both the nanosecond (Duguay and Hansen 1969b) and picosecond ranges (Laubereau 1969), no pulses shorter than the above limit of 4.10^{-13} sec were so far achieved in this way.

The presence of subpicosecond structure and frequency chirp in mode-locked Nd:glass lasers were the subject of some discussion in the literature. In particular, the model of mode-locking due to Picard and Schweitzer (1970) is able to explain the subpicosecond structure but it fails to explain the frequency chirp. On the other hand the model of Fisher and Fleck (1969) is able to explain the frequency chirp but it fails to explain the subpicosecond structure. Another interpretation of the frequency chirp should also be mentioned. Here the frequency chirp would be due to the nonlinear, intensity dependent refractive index either of the Q-switching dye solvent (Fisher et al. 1969) or of the laser glass matrix (Duguay et al. 1970). This model, too, fails to explain the subpicosecond structure. A model which appears to explain both the subpicosecond structure and frequency chirp was recently proposed by Svelto (1970). The model is an extension of a previously published theory of mode-locking which takes into account the dispersion of the refractive index of the media within the cavity, in particular of the laser material (Cubeddu and Svelto 1969). The theory indicates that the effect of dispersion strongly depends upon the total oscillating bandwidth. Since this bandwidth for ruby is about an order of magnitude smaller than for Nd:glass lasers, one now has theoretical reasons to expect no significant subpicosecond structure and frequency chirp for ruby. The problem is not yet completely solved, however, since even the model of Svelto (1970) is only in qualitative agreement with the recent results of Treacy (1970a, b). Furthermore, on the experimental side it is not yet clear, whether the same Nd^{3+}:glass laser gives always at the same time both a subpicosecond structure and a substantial frequency chirp or only one of these phenomena (Bradley et al. 1970).

References

ARECCHI, F. T. and R. BONIFACIO (1965), IEEE J. Quantum Electronics **1**, 169.
ARMSTRONG, J. A. (1967), Appl. Phys. Letters **10**, 16.
ASWAZADURIAN, N., S. RIVA, G. SONCINI and O. SVELTO (1968), J. Appl. Phys. **39**, 5928.

BASOV, N. G., P. G. KRIUKOV, V. S. LETOKHOV and YU. V. SENATSKII (1968), IEEE J. Quantum Electronics **4**, 606.
BEY, P. P., J. F. GIULIANI and H. RABIN (1968), Phys. Letters **26A**, 128.
BJORKHOLM, J. E. and R. H. STOLEN (1968), J. Appl. Phys. **39**, 4043.
BLOUNT, E. I. and J. R. KLAUDER (1969), J. Appl. Phys. **40**, 2874.
BORTFELD, D. P., R. S. CONGLETON, M. GELLER, R. S. MCCONAS, L. D. RILEY, W. R. SOWOY and M. L. STITCH (1964), J. Appl. Phys. **35**, 2267.
BRADLEY, D. J., G. H. C. NEW and S. J. CAUGHEY (1969), Phys. Letters **30A**, 78.
BRADLEY, D. J., G. H. NEW and S. J. CAUGHEY (1970a), Opt. Commun. **2**, 41.
BRADLEY, D. J., G. H. NEW and S. J. CAUGHEY (1970b), Phys. Letters **32A**, 313.
BRADLEY, D. J., T. MORROW, and M. S. PETTY (1970c), Opt. Comm. **2**, 1.
BRADLEY, D. J., B. LIDDY, and W. E. SLEAT (1971), Opt. Comm. **2**, 319.
BURNHAM, D. C. and K. W. BILLMAN (1968), Appl. Phys. Letters **13**, 419.
BURNHAM, D. C. (1970), Appl. Phys. Letters **17**, 45.
CLOBES, A. R. and N. J. BRIENZA (1969), Appl. Phys. Letters **14**, 287.
COMLY, J., E. GARMIRE, J. P. LAUSSADE and A. YARIV (1968), Appl. Phys. Letters **13**, 176.
CUBEDDU, R. and O. SVELTO (1969), IEEE J. Quantum Electronics **5**, 495.
CUBEDDU, R., R. POLLONI, C. A. SACCHI and O. SVELTO (1969), IEEE J. Quantum Electronics **5**, 470.
CUTLER, C. C. (1955), Proc. IRE **43**, 140.
DANEU, V., C. A. SACCHI and O. SVELTO (1966), IEEE J. Quantum Electronics **2**, 290.
DEMARIA, A. J., C. N. FERRAR and G. E. DANIELSON (1966a), Appl. Phys. Letters **8**, 22.
DEMARIA, A. J., D. A. STETSER and H. HEYNAU (1966b), Appl. Phys. Letters **8**, 174.
DEMARIA, A. J., R. GAGOSZ, H. A. HEYNAU, A. W. PENNEY and G. WISNER (1967), J. Appl. Phys. **38**, 2693.
DEMARIA, A. J., W. H. GLENN, H. J. BRIENZA and M. E. MACK (1969), Proc. IEEE **57**, 2.
DEUTSCH, T. (1965), Appl. Phys. Letters **7**, 80.
DIDOMENICO, M., J. E. GEUSIC, H. N. MARCOS and R. G. SMITH (1966), Appl. Phys. Letters **8**, 180.
DUGUAY, M. A. and J. W. HANSEN (1969a), Opt. Commun. **1**, 254.
DUGUAY, M. A. and J. W. HANSEN (1969b), Appl. Phys. Letters **14**, 14.
DUGUAY, M. A., J. W. HANSEN and S. L. SHAPIRO (1970), IEEE J. Quantum Electronics **6**, 725.
DUNSMUIR, R. (1961), J. Electronics and Control (GB), **10**, 453.
ECKARDT, R. C. and C. H. LEE (1969), Appl. Phys. Letters **15**, 425.
ERICKSON, L. E. and A. SZABO (1966), J. Appl. Physics **37**, 4953.
FISHER, R. A., P. L. KELLEY and T. K. GUSTAFSON (1969), Appl. Phys. Letters **14**, 140.
FISHER, R. A. and J. A. FLECK (1969), Appl. Phys. Letters **15**, 287.
FLECK, J. A. (1968), Appl. Phys. Letters **12**, 178.
GARMIRE, E. and A. YARIV (1967), IEEE J. Quantum Electronics **3**, 222.
GIORDMAINE, J. A., P. M. RENTZEPIS, S. L. SHAPIRO and K. W. WECHT (1967), Appl. Phys. Letters **11**, 216.
GIORDMAINE, J. A., M. A. DUGUAY and J. W. HANSEN (1968), IEEE J. Quantum Electronics **4**, 252.
GIRES, F. and P. TOURNOIS (1964), Compt. Rend. **258**, 6112.
GIULIANO, C. R. and L. D. HESS (1967), IEEE J. Quantum Electronics **3**, 358.
GLENN, W. H. and M. J. BRIENZA (1967), Appl. Phys. Letters **10**, 221.
HARGROVE, L. E., R. L. FORK and M. A. POLLACK (1964), Appl. Phys. Letters **8**, 22.
HARRACH, R. and G. KACHEN (1968), J. Appl. Phys. **39**, 2482.
HARRIS, S. E. and R. TARG (1964), Appl. Phys. Letters **5**, 202.
HARRIS, S. E. and O. P. MCDUFF (1965), IEEE J. Quantum Electronics **1**, 245.
HELLWARTH, R. W. (1961), in: Advances in Quantum Electronics (J. R. Singer, ed.; Columbia University Press; New York), 334.
HELLWARTH, R. W. (1966), in: Lasers, vol. 1 (A. K. Levine, ed.; Marcel Dekker; New York), 253.
HERCHER, M. (1965), Appl. Phys. Letters **7**, 39.
HERCHER, M., W. CHU and D. L. STOCKMAN (1968), IEEE J. Quantum Electronics **4**, 954.
HOOK, W. R., R. H. DISHINGTON and R. P. HILBERG (1966), Appl. Phys. Letters **9**, 125.
KACHEN, G., L. STEINMETZ and J. KYSILKA (1968), Appl. Phys. Letters **13**, 229.
KLAUDER, J. R., M. A. DUGUAY, J. A. GIORDMAINE and S. L. SHAPIRO (1968), Appl. Phys. Letters **13**, 174.
KLEINMAN, D. A. and P. P. KISLIUK (1962), Bell Syst. Tech. J. **41**, 453.

KOROBKIN, V. V. and M. Ya. SCHELEV (1968), in: High Speed Photography, (ed. by N. R. Nilsson and L. Hogberg; Stockholm), 36.
KRASYUK, I. K., P. P. PASHININ and A. M. PROKHOROV (1968), Soviet Phys. JETP Letters **7**, 89.
KUIZENGA, D. J. and A. E. SIEGMAN (1970a), IEEE J. Quantum Electronics, **6**, 694.
KUIZENGA, D. J. and A. E. SIEGMAN (1970b) IEEE J. Quantum Electronics, **6**, 709.
KUZNETSOVA, T. I., V. I. MALYSHEV and A. S. MARKIN (1967), Soviet JETP **25**, 286.
LAMB, W. E. Jr. (1964), Phys. Rev. **134**, A1429.
LAUBEREAU, A. (1969), Phys. Letters **29A**, 539.
LENGYEL, B. A. (1966), Introduction to Laser Physics (John Wiley and Sons; New York), 235.
MACK, M. E. (1968a), IEEE J. Quantum Electronics **4**, 1015.
MACK, M. E. (1968b), J. Appl. Phys. **39**, 2483.
MAIER, M., W. KAISER and J. A. GIORDMAINE (1966), Phys. Rev. Letters **17**, 1275.
MANGER, H. and H. ROTHE (1963), Phys. Letters **7**, 330.
MCDUFF, O. P. and S. E. HARRIS (1967), IEEE J. Quantum Electronics **3**, 101.
MCCLUNG, F. J. and D. WIENER (1965), IEEE J. Quantum Electronics **1**, 94.
MICHON, M., J. ERNEST and R. AUFFRET (1966), Phys. Letters **21**, 514.
MIKAELIAN, A. L., Yu. G. TURKOV and V. G. SAVEL'EV (1967), Sov. Phys. JETP Letters **6**, 161.
MOCKER, H. W. and R. J. COLLINS (1965), Appl. Phys. Letters **7**, 270.
PENNEY, A. W. and H. A. HEYNAU (1966), Appl. Phys. Letters **9**, 257.
PICARD, R. H. and P. SCHWEITZER (1970), Phys. Rev. **A1**, 1803.
RENTZEPIS, P. M. and M. A. DUGUAY (1967), Appl. Phys. Letters **11**, 218.
RENTZEPIS, P. M., C. J. MITSCHELE and A. C. SAXMAN (1970), Appl. Phys. Letters **17**, 122.
ROESS, D. (1964), Proc. IEEE **52**, 196.
SACCHI, C. A., G. SONCINI and O. SVELTO (1967), Nuovo Cimento **48**, 58.
SCARLET, R. I., J. F. FIGUERIA and H. MAHR (1968), Appl. Phys. Letters **17**, 71.
SCHWARZ, S. E. (1968), IEEE J. Quantum Electronics **4**, 509.
SCHWARZ, S. E. and P. L. GORDON (1969), J. Appl. Phys. **40**, 4441.
SHAPIRO, S. L. and M. A. DUGUAY (1969), Phys. Letters **28A**, 698.
SHELTON, J. W. and J. A. ARMSTRONG (1967), IEEE J. Quantum Electronics **3**, 696.
SIEGMAN, A. E. and K. J. KUIZENGA (1969), Appl. Phys. Letters **14**, 181.
SIEGMAN, A. E. and D. J. KUIZENGA (1970), IEEE J. Quantum Electronics, **QE-6**, 803.
SMITH, P. W. (1965), IEEE J. Quantum Electronics **1**, 343.
SONCINI, G. and O. SVELTO (1967), Appl. Phys. Letters **11**, 261.
SONCINI, G. and O. SVELTO (1968), IEEE J. Quantum Electronics **4**, 422.
SOOY, W. R. (1965), Appl. Phys. Letters **7**, 36.
STATZ, H. and G. DEMARS (1960), in: Quantum Electronics (C. H. Townes, ed.; Columbia University Press; New York), 530.
STATZ, H. and C. L. TANG (1965), J. Appl. Phys. **36**, 3928.
STATZ, H., G. A. DE MARS and C. L. TANG (1967), J. Appl. Phys. **38**, 2212.
SVELTO, O. (1970), Appl. Phys. Letters **17**, 83.
SZABO, A. and R. A. STEIN (1965), J. Appl. Phys. **36**, 1562.
TANG, C. L. and H. STATZ (1967), J. Appl. Phys. **38**, 2963.
TREACY, E. B. (1968), Phys. Letters **28A**, 34.
TREACY, E. B. (1969), Appl. Phys. Letters **14**, 112.
TREACY, E. B. (1970a), Appl. Phys. Letters **17**, 14.
TREACY, E. B. (1970b), to be published.
VON DER LINDE, D., O. BERNECKER, and A. LAUBEREAU (1970), Opt. Comm. **2**, 215.
VUYLSTEKE, A. A. (1963), J. Appl. Phys. **34**, 1615.
WAGNER, W. G. and B. A. LENGYEL (1963), J. Appl. Phys. **34**, 2040.
WEBER, H. P. (1967), J. Appl. Phys. **38**, 2231.
WEBER, H. P. (1968a), J. Appl. Phys. **39**, 6041.
WEBER, H. P. (1968b), Phys. Letters **27A**, 321.
WEBER, H. P. and R. DÄNDLIKER (1968), Phys. Letters **28A**, 77.